Fluorescent Semiconducting Polymer Conjugates of Poly(*N*-isopropylacrylamide) for Thermal Precipitation Assays

Kenichi Kuroda and Timothy M. Swager*

Department of Chemistry, Massachusetts Institute of Technology, Cambridge, Massachusetts 02139

Received September 13, 2003; Revised Manuscript Received December 8, 2003

ABSTRACT: New thermally responsive fluorescent polymers conjugated with poly(*N*-isopropylacrylamide) (polyNIPA) have been synthesized. A nonionic water-soluble poly(phenylene−ethynylene) (PPE) was end-capped with a di-*tert*-butylnitroxide derivative, and subsequent nitroxide-mediated radical polymerization of NIPA afforded PPE−polyNIPA block copolymers. These copolymers phase-separate from aqueous solutions upon heating, and the resultant precipitates are efficiently collected by filtration. The fluorescent spectra of the precipitates indicate the absence of strong associations between the PPE π-systems. Furthermore, the fluorescent intensities of the collected solids have a linear correlation with the polymer concentrations in the solutions of origin. When copolymers are thermally coprecipitated with dye-labeled (rhodamine B) polyNIPA materials, the dye is localized to the PPE segments, inducing fluorescent resonance energy transfer from the PPE segment (donor) to the dye (acceptor).

Introduction

Fluorescent semiconducting polymers (FSPs) have emerged as a powerful class of sensory materials[1] and have enabled the formation of ultrasensitive sensors for explosive molecules,[2−4] metal ions,[5−8] and biomolecules.[9−13] The delocalized π-electrons in the polymer's backbone create energy bands and facilitate the transport of excited states (excitons).[14] This transport allows excitons to visit many potential binding sites that may be occupied by an analyte molecule that is capable of inducing fluorescence quenching or a new emission feature. This long-distance exciton transport produces the signal amplification that allows for ultrasensitive sensory responses.[15]

A variety of different detection mechanisms have been developed to translate analyte binding to fluorescent sensory responses. These include electron-transfer quenching by paraquat bound to receptor sites,[16] π-complexation with nitroaromatics such as trinitrotoluene (TNT),[2,3] energy transfer to activated indicators,[17] analyte-initiated aggregation of FSPs,[7] and coordination to pyridyl ligands by transition metal ions.[6,18] To extend the utility of FSPs as sensory materials, new transduction schemes making use of conjugated polyelectrolytes have been investigated.[9−13] DNA detection has been recently demonstrated[9,10] utilizing FSP amplified fluorescence resonance energy transfer (FRET).[17] This DNA detection scheme makes use of the well-known distance dependence of FRET that is the basis of many biosensory transduction schemes with cationic FSPs electrostatically binding to DNA.[13] The localization of the FSP and a fluorescent DNA probe results in efficient FRET. However, few other biosensory schemes can rely on such strong ionic associations. A concern is that those systems having weaker molecular recognition elements may suffer from nonspecific electrostatic associations. Hence, in ionic FSP biosensory systems, the sensory responses will likely be limited to conditions wherein solutions contain only a few species of analytes, thereby producing less interference in analysis. Clearly, it is advantageous to develop new nonionic systems that are capable of analyzing complex unprocessed biological fluids that contain a variety of analytes and charged biomolecules.

Considering the anticipated limitations of ionic FSP biosensors, we are seeking to develop a new transduction scheme which would (1) make use of water compatible FSPs to allow biomolecular recognition events take place in solution, (2) employ nonionic FSPs that are immune to indiscriminate electrostatic interactions, (3) maximize the signal amplification resulting from energy migration in FSPs, and (4) allow selective collection of sensory FSPs from analyte solutions in order to remove interferants and facilitate fluorescence measurements. To this end we report herein a thermally responsive block polymer of a nonionic water-soluble poly(phenylene−ethynylene)[19] (PPE) and poly(*N*-isopropylacrylamide) (polyNIPA), **P-I** (Chart 1). The polyNIPA block produces phase separation upon heating (>30 °C) due to a hydrophobic collapse mechanism.[20] To investigate the potential of **P-I** for use in sensory schemes, we have demonstrated that thermal coprecipitation with dye−polyNIPA conjugate **P-II** (Chart 1) induces FRET from the PPE segment to the dye.

Results and Discussion

Synthesis and Characterization of an FSP−PolyNIPA Conjugate. The FSP−polyNIPA conjugate (**P-I**) was synthesized from a water-soluble PPE end-capped with an alkoxyamine capable of initiating nitroxide-mediated radical polymerization (NMRP) of NIPA to give a block copolymer. The synthesis of the end-capping/NMRP initiator **3** (Scheme 1) begins with compound **1** obtained from treatment of 4-iodobenzoyl chloride and an excess amount of 2,2′-(ethylenedioxy)-bis(ethylamine), and a subsequent reaction with 2-chloropropionyl chloride produces **2**. We have adapted methods developed by Matyjaszewski to afford **3**,[21] wherein compound **2** reacts with CuCl to produce a radical that is captured by the di-*tert*-butyl nitroxide radical to give **3**. A competitive process is the back-reaction of the radical with $CuCl_2$/Me_6TREN to regenerate **2**. This process is attenuated by the addition of

* Corresponding author: e-mail tswager@mit.edu.

10.1021/ma035373+ CCC: $27.50
Published on Web 01/16/2004

Chart 1

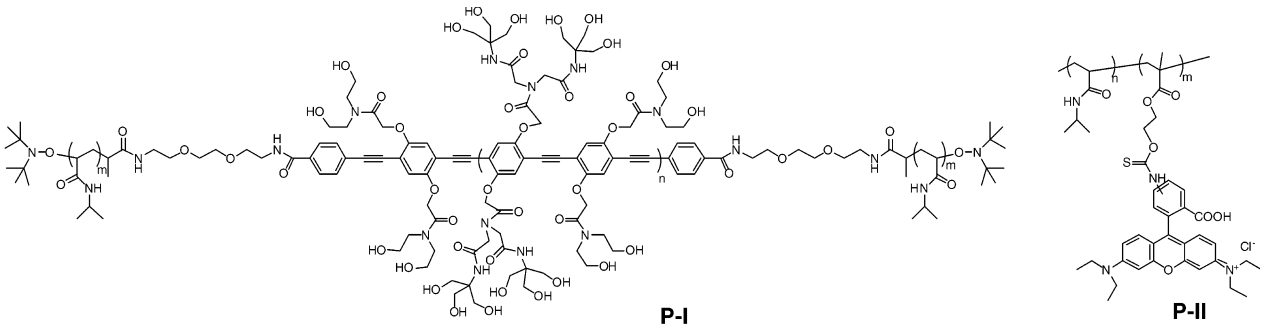

Scheme 1

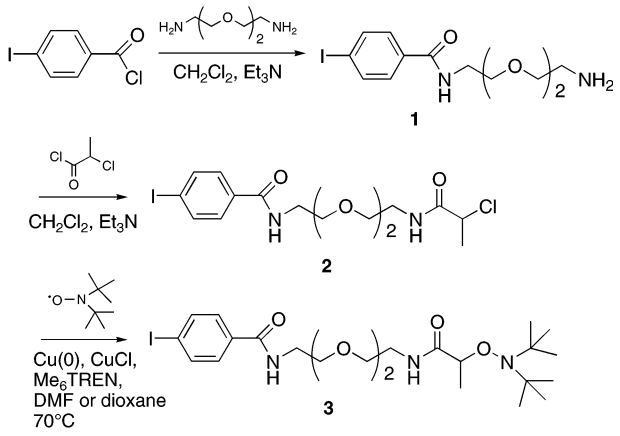

Cu(0), which reduces the Cu(II) spices that serve to regenerate **2** and thereby drives the reaction to completion.

The water-soluble PPE **6** in Scheme 2 was synthesized from monomers **4** and **5**[19] and the end-capping/NMRP initiator **3** by a Sonogashira cross-coupling using a Pd catalyst and CuI cocatalyst in morpholine. This polymer was purified by precipitation in ethyl acetate and dialysis against water and was then isolated by lyophilization. NMR analysis provided the degree of polymerization (DP) by integrating the signals from the aromatic and amide groups in the PPE relative to those from the *tert*-butyl moieties of the end-caps that are well-resolved from other polymer signals. The DP of **6** was found to be 11.5. Gel permeation chromatography (GPC) analysis indicated that M_n, M_w, and polydispersity index (PDI) of purified **6** are 23 556, 34 411, and 1.46, respectively.

The NMRP of NIPA was carried out using **6** as an initiator in DMF or DMSO at 120 °C. The resultant polymer was purified by precipitation in diethyl ether and dialysis against water. Generally, in the NMRP mechanism, the weak C−O bond of alkoxyamine initiator homolyzes to give a nitroxide radical and a carbon radical.[22] The carbon radical then initiates radical polymerization, and in an ideal case, a polymer chain grows without termination reactions, thereby enabling the synthesis of multiblock copolymers.[23,24] Previous studies on the NMRP process have revealed the importance of the nitroxide's (alkoxyamine's) structure to control reactivity in the radical polymerization process.[22,25] Consistently we found that the 2,2,6,6-tetramethyl-1-piperdinyloxyl (TEMPO)-based initiator gave no polymer. However, the di-*tert*-butyl nitroxide derivative initiator (**3**) worked well to produce polyNIPA. The di-*tert*-butyl nitroxide initiator has higher reactivity than the TEMPO initiator due to its steric hindrance which weakens the C−O bond, thereby lowering the temperatures required for polymerization.[26−28] Despite the use of NMRP, GPC analysis of the block copolymer **P-I** showed a bimodal elution profile with a broad molecular weight distribution (M_n = 51 604, M_w = 233 100, PDI = 4.52), which suggests that the resultant polymer contains tri- and diblock copolymers. The observed polydispersity is likely due to chain termination events. Control experiments initiating NMRP of NIPA using only initiator **3** with monomer-to-initiator ratios of 100

Scheme 2

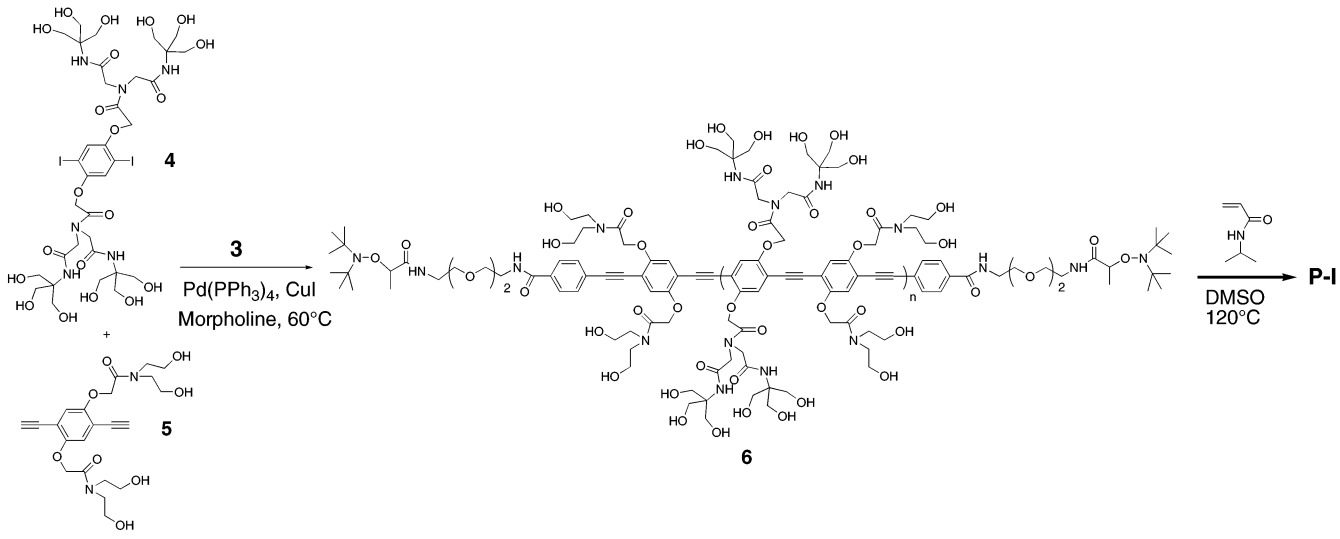

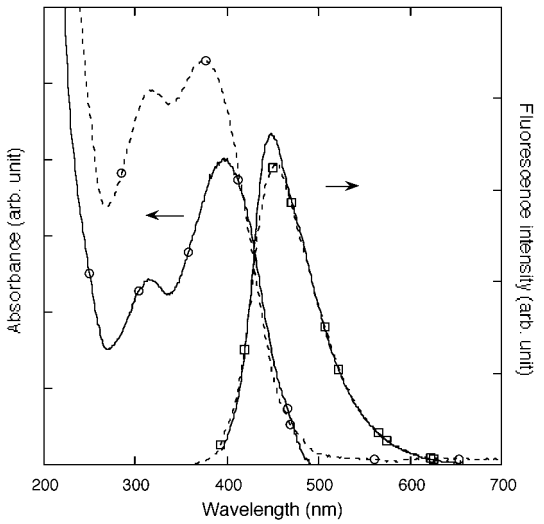

Figure 1. UV−vis absorption and fluorescence spectra of PPE **6** (solid lines with circles and with squares) and **P-I** (broken lines with circles and with squares). The excitation wavelengths for the fluorescence spectra are 380 nm for **6** and 350 nm for **P-I**.

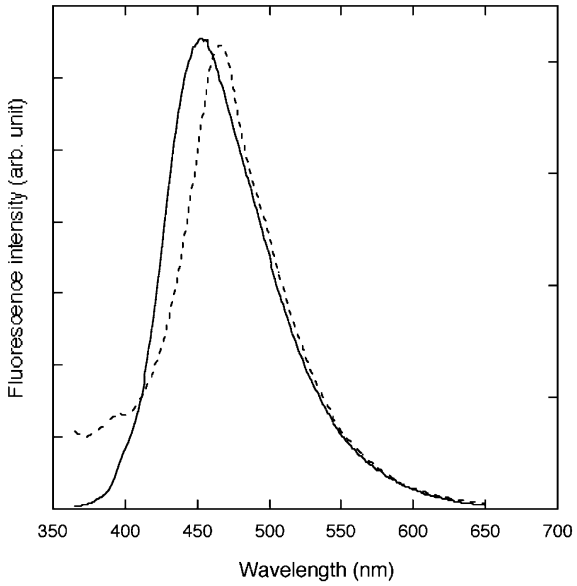

Figure 2. Fluorescence spectra of **P-I** in solution (solid line) and solid on a filter paper (broken line). The excitation wavelength is 350 nm.

gave a DP of 42 by ^{1}H NMR and yields of 14%. (M_n, M_w, and PDI are 18 349, 25 745, and 1.4, respectively, by GPC.) Precise polymerizations of NIPA are generally difficult, and only Harth et al. have obtained polyNIPA by the NMRP method with accurately controlled molecular weights and low polydispersities by using specially designed initiators.[29] We investigated a related ATRP method that has been successful for the formation of short conjugated oligomer−polystyrene block copolymers with low polydispersity.[30] This method makes use of oligo(*p*-phenylene−ethynylene)s end-capped with ATRP initiators at their termini and subsequent polymerization of styrene using a CuBr catalyst. We attempted to end-cap PPE **6** with **2** as an ATRP initiator by the same procedure in Scheme 2. However, we found that **2** was not stable to the Sonogashira polymerization conditions. Given that the observed polydispersity of **P-I** does not present obvious limitations to the present study and the resultant copolymer is highly water-soluble and thermally precipitates upon heating, we have completed the following studies with our high-PDI samples.

The UV−vis absorption spectra of **P-I** and the precursor PPE **6** are shown in Figure 1. After copolymerization by the NMRP method, a blue shift in **P-I**'s absorption spectra was observed, whereas its fluorescence showed no shift. A plausible explanation for the blue shift in the absorption spectrum is that the polyNIPA block disturbs the π-conjugation of the PPE segments and creates a higher energy gap in their electronic structure. The lack of change in the fluorescence is likely due to energy migration from the terminal portions of the PPE that are more affected by the polyNIPA to the center of the PPE. In this way, the emission corresponding to the lower energy gap in the center of the PPE dominates the spectrum, and it appears to be the same as that of **6**.

Thermally Induced Precipitation. We are interested in developing sensor assays that make use of the phase separation from aqueous solution upon heating. To this end we examined a scheme whereby polymers are collected as solid precipitates to remove interferants and to facilitate analysis. To prepare completely soluble polymer aqueous solutions, the polymers were stirred in an ice bath. At these temperatures the polyNIPA chains dissociate and are completely solvated by water. Fluorescent assays are best performed at concentrations lower than typically used in the precipitation of polyNIPA, and in order to effect quantitative phase separation, aqueous NaCl was added to the polymer solutions.[20] The addition of salt is well-known to reduce the phase separation temperature.[20,31] The polymer solutions (polymer concentrations 0.25−0.025 mg/mL) were heated at 50 °C, and the resultant precipitate was collected by vacuum filtration with a small filter paper (diameter 8 mm) on a Hirsch funnel and washed with hot water to remove the salts. The filtrate had a slight yellow color and blue fluorescence. It appears that only trace amounts of the polymer passed though the filter paper. After drying under vacuum at room temperature, the filter paper was placed between a coverslip and a glass microscope slide, and its fluorescence was measured. This procedure was reproduced many times, and we found that the reproducibility of the emission intensities was within 20%, which provides useful analysis in many potential biosensory assays.

The fluorescence spectra of **P-I** on a filter paper (Figure 2) reveal a slight red shift in the emission relative to that in solution, and there are no new emission signals. The fact that the emission band shape is largely the same in the precipitate as in solution is consistent with the absence of strong interchain π-associations (aggregation) that produce broad new low-energy and undesired weakly emitting bands.[32] Aggregation of conjugated polymers is generally enhanced in the solid state because of the potential of interchain $\pi-\pi$ stacking. Hence, the absence of such features indicates that the polymer chains are largely prevented from having strong interchain electronic interactions, perhaps due to the dendritic side chains of **P-I**.

The fluorescence spectra of the polymer (**P-I**) precipitates were measured with variable polymer concentrations (Figure 3), and the emission intensity from the polymers collected on the filter papers increased linearly with increasing polymer concentrations. These results confirm that our collection method using filter paper accurately reflects the polymer concentration in solu-

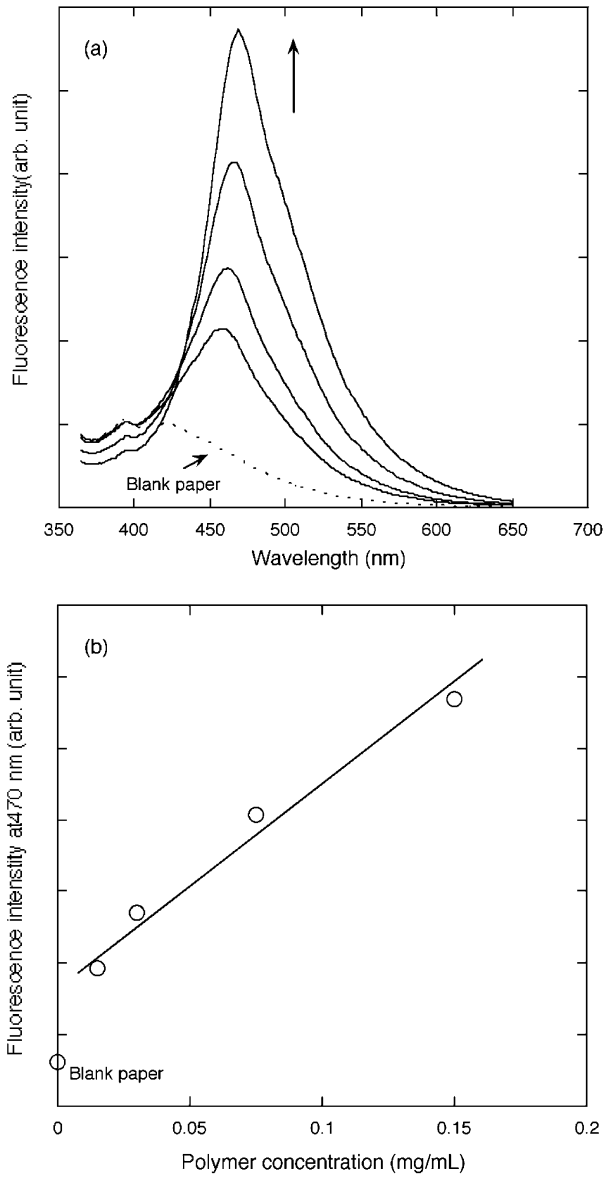

Figure 3. Fluorescence spectra of **P-I** on filter papers (a) and intensities at 470 nm (b). The intensity increases with increasing the polymer concentration (0.015, 0.03, 0.075, and 0.15 mg/mL). The excitation wavelength is 350 nm.

tion. As can be seen in Figure 3, the polymer emission peak is slightly red-shifted with increasing polymer concentrations. This is likely due to a spectral overlap of strong background scattering from the filter paper and the polymer emissions, which results in an apparent red shift with the increase of the polymer emission.

Thermal Precipitation Induced Energy Transfer. Through-space fluorescence resonance energy transfer (FRET) is a distance-dependent dipolar interaction of chromophores (a donor and acceptor) and is widely used in sensory transduction schemes and assays for the detection of biomolecules. In the FRET (Förster) mechanism, the energy of the excited donor is efficiently transferred to the acceptor without emission when they are within the Förster radius (of 50−100 Å) of each other.

Our interest was to examine whether the thermally induced phase separation of **P-I** can trigger FSP-amplified FRET with dye molecules. The advantage of this process is that the emission intensity from an acceptor dye molecule can be enhanced by energy

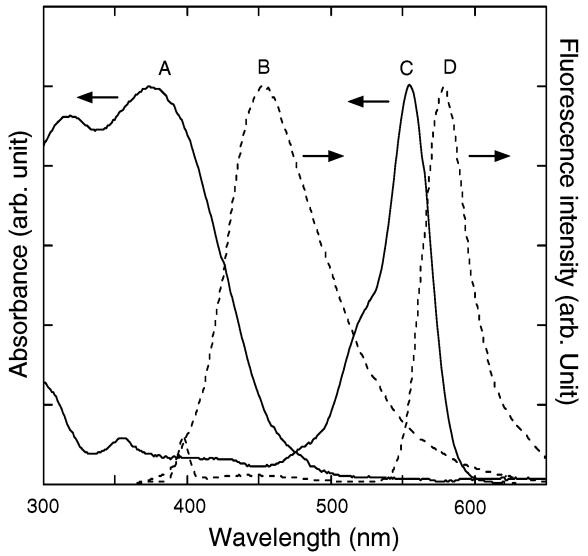

Figure 4. Normalized UV−vis absorption and fluorescence spectra of **P-I** (A and B) and **P-II** (C and D) in water with excitation at 350 nm.

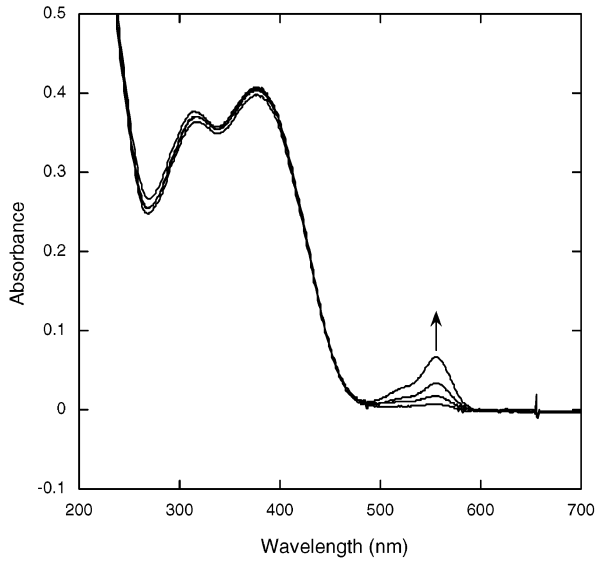

Figure 5. Absorption spectra of solution mixtures of **P-I** and **P-II**. **P-I** concentration was constant at 0.12 mg/mL. **P-II** concentrations are 0.05, 0.025, 0.0125, and 0.00625 mg/mL, and the absorbance at 560 nm increased with increasing **P-II** concentrations.

transfer from the donor FSP which can capture a larger percentage of the excitation photons due to its greater optical cross-section.[10,17] To test this approach, a dye−polyNIPA conjugate **P-II** was prepared by a free radical copolymerization of NIPA with a rhodamine B (RhB) methacrylate monomer using AIBN in DMF (M_n = 86 909, M_w = 142 730, and PDI = 1.64 by GPC).

Normalized UV−vis absorbance and fluorescence spectra of **P-I** and **P-II** in water are shown in Figure 4. The spectral overlap of the PPE (donor) emission from **P-I** and the RhB (acceptor) absorption from **P-II** was chosen to produce efficient FRET based on the Förster mechanism and to also give an acceptor emission that is well-resolved from that of **P-I,** thereby facilitating analysis.

The absorption and fluorescence spectra from mixed solutions of **P-I** and **P-II** are shown in Figure 5 and Figure 6, respectively. When the solution was excited

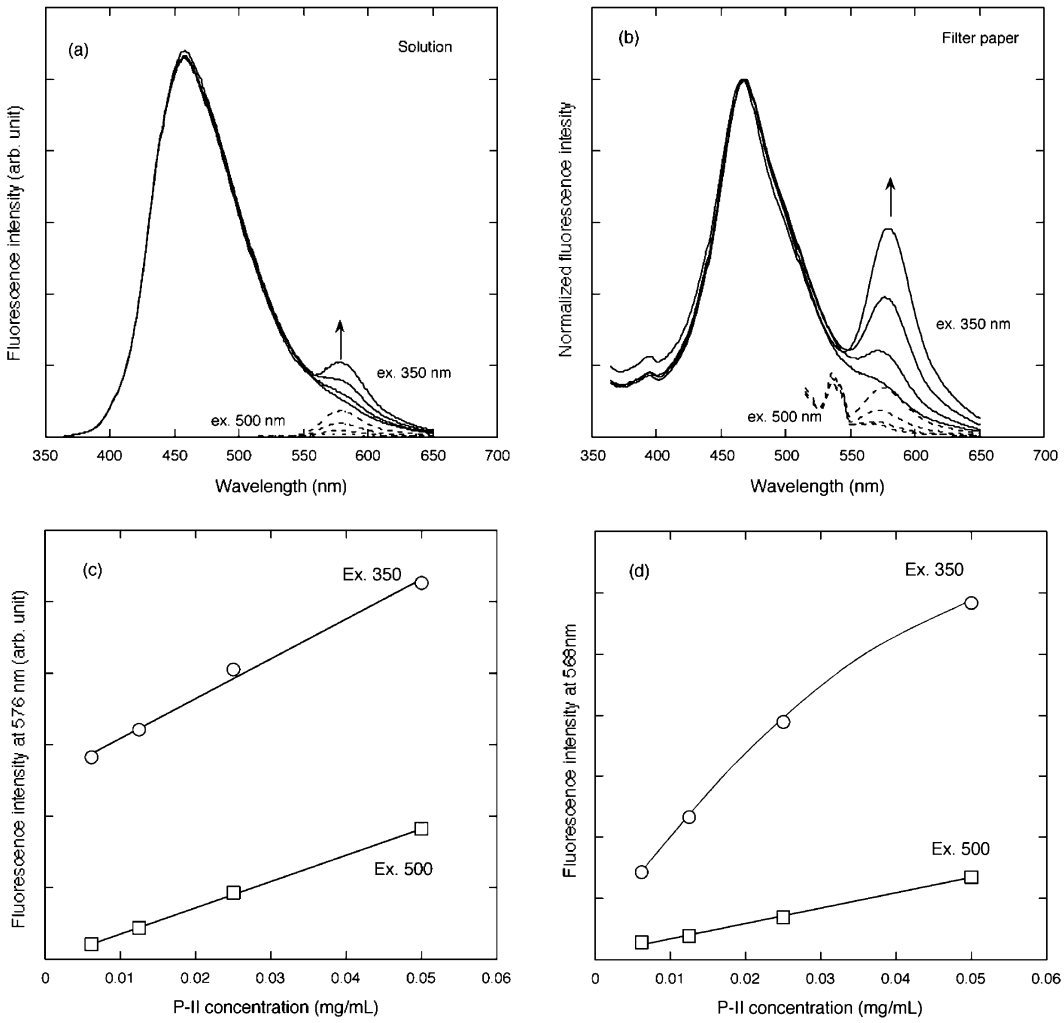

Figure 6. Fluorescence spectra of the mixture of **P-I** and **P-II** in a solution (a) and on a filter paper (b). The spectra in (b) are normalized relative to the peak intensities at 468 nm. **P-I** concentration in the solutions was 0.12 mg/mL. **P-II** concentrations are 0.05, 0.025, 0.0125, and 0.00625 mg/mL in the solutions. **P-I** is the principal absorbing group with 350 nm excitation, and **P-II** is selectively excited with excitation at 500 nm. Light scattering from the filter paper gives a peak at 540 nm in (b). Fluorescence intensity at 580 nm increased with higher **P-II** concentrations. The solid lines in (c) and (d) show the dependence of the different emissions as a function of **P-II** concentration.

at 350 nm, a major emission peak from the PPE segments of **P-I** and a small one from the RhB bound to **P-II** were observed at 470 and 580 nm, respectively. With excitation at 500 nm, the RhB was selectively excited, and its emission was observed at 580 nm. The fluorescence intensity from RhB in solution at both excitation wavelengths was found to be directly proportional to the **P-II** concentration (Figure 6c). The ability to directly excite the RhB thereby allows this signal to be used as an internal reference to its concentration.

Thermally precipitated mixtures of **P-I** and **P-II** were collected on a nonfluorescent filter paper using procedures described earlier, and the normalized fluorescence spectra from the filter paper are shown in Figure 6. We find that the emission at 580 nm from the RhB is 5 times larger when we excited principally the PPE at 350 nm than when we selectively excited the RhB at 500 nm. This effect is not due to the differences of the excitation intensities at the excitation wavelengths because the photon fluxes with excitation at 350 and 500 nm are corrected to be the same by the spectrometer. In this experiment the RhB was excited at 500 nm rather than its absorption maximum to avoid an overlap with strong light scattering from the filter paper. We have further determined that the quantum yield of precipitated **P-I** is independent of added polyNIPA. Therefore, the increasing emission from RhB with excitation at 350 nm is due to FRET induced by thermal precipitation that localizes the RhB molecules to the vicinity of the PPE segments. The RhB absorbance maximum is at 560 nm, and on the basis of the differences in excitation coefficient at 500 nm, we would expect the emission to be 4 times larger than that obtained with 500 nm excitation. As a result, in terms of practical signal gains for sensory assays this system only yields enhancements of about 20%. Nevertheless, we emphasize that comparisons with the solution data validate that thermal precipitation induces FRET. The linear dependence on **P-II** concentration in the emission intensity from the RhB with excitation at 500 nm in the coprecipitates confirms, similar to **P-I**, that our precipitation assay is quantitative and reflects the true concentration of the polymer in solution (Figure 6d). Interestingly, the RhB fluorescence intensity at 580 nm from the filter papers ($\lambda_{ex} = 350$ nm) slightly levels off with increasing the **P-II** concentrations (Figure 6d). This is an additional signature of energy transfer and is due to the fact that at high RhB concentrations there

Chart 2

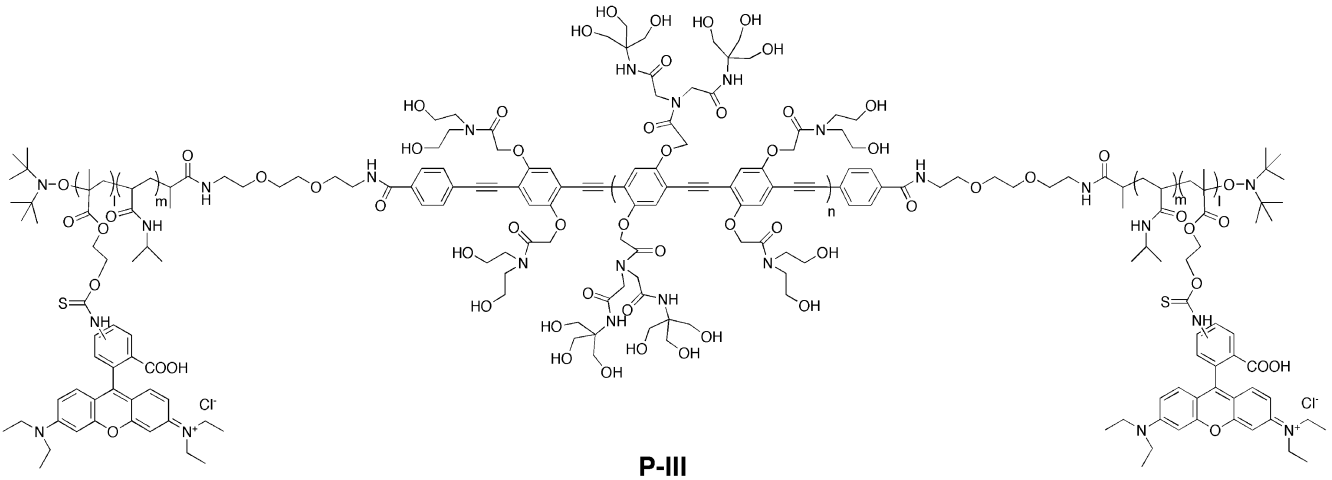

P-III

are multiple RhB acceptors within the Förster radius and diffusion range of an exciton. In this way, the amount of energy available to each RhB acceptor from the PPE donors decreases, leading to leveling-off of the RhB emission intensity.

Despite our successful demonstration of thermal precipitation induced energy transfer from **P-I** to **P-II**, there are a number of features that indicate that FRET processes lack the efficiency that would be required for a viable assay. First, we are only able to increase the RhB emission about 20% beyond that which can be obtained by the optimal direct excitation of this dye. Second, the donor (PPE) emission does not decrease significantly with increasing RhB concentrations, which indicates that only a small amount of the donor's energy is being captured by the acceptor. We have considered that the inefficiency in energy transfer from the PPE segments can be attributed to one or more of the following issues: (1) The polymers have different phase separation temperatures, resulting in the polymers precipitating separately into macrophase-separated domains. (2) The RhB is imbedded in polyNIPA aggregates and located too far from the PPE segments. (3) The spectral overlap of the PPE emission and the RhB absorption is not optimal (Figure 4). (4) The PPE segment of **P-I** has a relatively low quantum yield, which could be attributed to a weak aggregation of the polymers.[19] We can rule out the possibility of phase separation by very rapidly heating the polymer mixtures, and the lack of any significant differences suggests that this is not a consideration. The fact that the PPE block polymer may microphase separate from **P-II** was addressed by synthesizing a block copolymer with polyNIPA blocks randomly containing a RhB comonomer (**P-III**, Chart 2). The incorporation of the dye into the copolymer structure should work to better compatibilize the two materials. The absorption spectrum (Figure 7) suggests that a small amount of RhB relative to the PPE segment is incorporated into the polyNIPA block of **P-III**, which is comparable to the mixtures of **P-I** and **P-II** (Figure 5). The precipitation assay using **P-III** was performed by the same procedure as **P-I**. As can be seen in Figure 8, the intensity ratio of the RhB emission excited at 350 nm to that excited at 500 nm is about 5, which is almost same order of enhancement as the mixture of **P-I** and **P-II** in Figure 6, indicating still lack of highly efficient FRET.

To produce a higher spectral overlap, we also considered different fluorescent dyes as FRET partners. Mc-

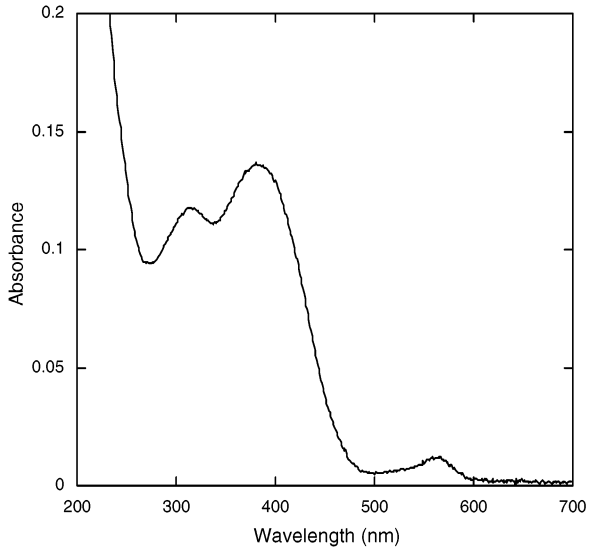

Figure 7. Absorption spectrum of **P-III** in water.

Quade et al. reported highly efficient amplified emissions from fluorescein by FRET from PPE thin films.[17] In this case fluorescein has the advantage of a larger spectral overlap with the PPE than RhB. However, when the same experiments are carried out with a fluorescein conjugate of polyNIPA, we observe a dramatic reduction in the emission from fluorescein with precipitation. This loss of emission is likely the result of the hydrophobic environment in the polyNIPA precipitates, which induces the conversion of this dye to its colorless and nonfluorescent lactone. The low quantum yields of these polymers are clearly a limitation, and enhancing the emission efficiencies of our nonionic water-soluble polymers is a challenging and ongoing research goal.

Summary

New thermally responsive PPE conjugates of polyNIPA have been synthesized, which precipitate from aqueous solution upon heating, resulting in the isolation of PPE for facile fluorescence measurements. A thermally induced coprecipitation of these copolymers with a RhB–polyNIPA conjugate induces FRET from PPE to RhB. While this method presently lacks the necessary performance to produce high amplification desired for biological sensing, we have developed general proce-

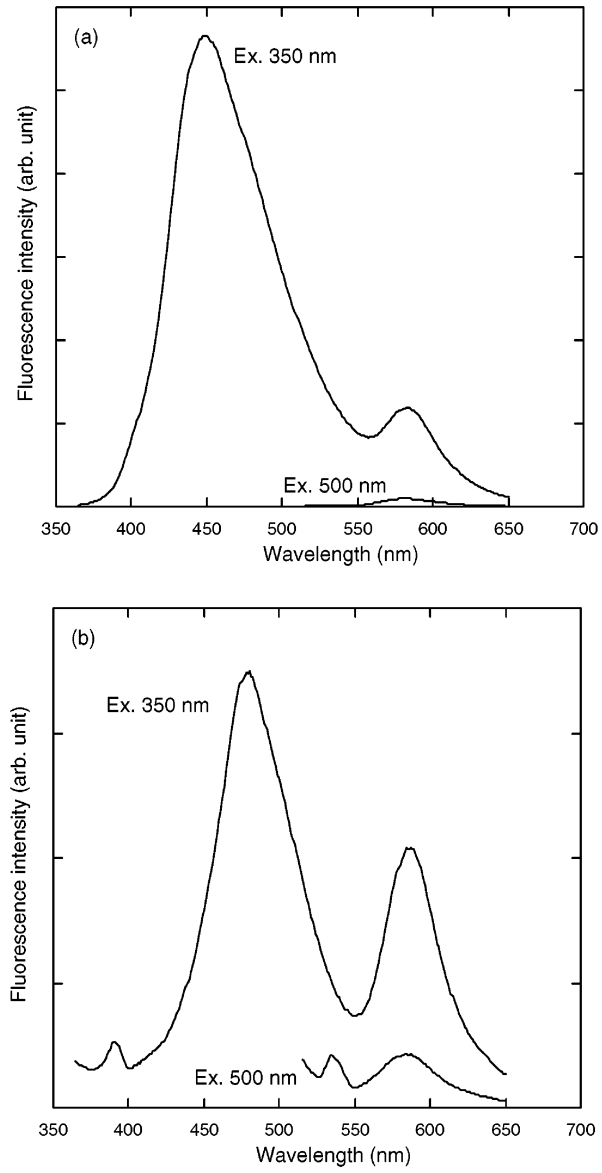

Figure 8. Fluorescence spectra of **P-III** solution (a) and a filter paper (b). The emission at 540 nm in the spectra (excitation at 500 nm) (b) is light scattering from the filter paper.

dures and synthetic methods that can be applied to other optimized systems. Our ongoing efforts are in progress, directing at solving the problems encountered, which include efficient localization of dye molecules to FSP segments by thermal precipitation, reductions in self-quenching by aggregation of FSPs, increased spectral overlaps of FSPs (donors) and dyes (acceptors), and the design of new nonionic water-soluble polymers. It is further anticipated that in some circumstances even nonionic water-soluble polymers can exhibit nonspecific weak binding of biomolecules and methods to prevent, or mitigate the effects of, entrapment of these species in thermally precipitation assays will need to be addressed.

In this report, we made use of a dye−polyNIPA conjugate as a simple model analyte to examine the basic assay principle. We also envision that improved assays can make use of FSP−polyNIPA conjugates in bioassay schemes with polyNIPA conjugates of antibodies, enzymes, and DNAs.[33−35] These polyNIPA bioconjugates will provide molecular recognition of analytes, including antibody−antigen coupling and DNA base pair matching. Once the target analytes (antigens or DNAs) are captured by polyNIPA bioconjugates, thermally induced coprecipitation with FSP−polyNIPA conjugates will be performed, and the analytes can be quantified by FSP-amplified fluorescent detection. This thermal precipitation assay method with bioconjugates of polyNIPA offers a new transduction scheme for FSP-based biosensors.

Experimental Procedures

General. Fluorescence spectra were measured on a SPEX Fluorolog-τ2 spectrofluorometer. CuCl was purified by stirring in acetic acid overnight. The remaining solid was filtered, washed with EtOH, dried under vacuum, and stored under Ar. NMR spectra were obtained on Varian Unity or Mercury 300 spectrometer. High-resolution mass spectra were obtained at the MIT Department of Chemistry Instrumentation Facility (DCIF) on a Bruker Daltronics APEX II 3 T FT-ICR-MS. Polymer molecular weights were determined with a Agilent 1100 series HPLC equipped with a PL gel 5 μm guard column and three columns (PL gel 5 μm, 10^5 Å, 10^4 Å, 10^3 Å) connected in series using DMF containing 5 mM BuLi as an eluent. GPC measurements were made relative to monodisperse polystyrene standards using a refractive index detector. The synthesis of the monomers **4** and **5** was reported previously.[19]

***N*-{2-[2-(2-Aminoethoxy)ethoxy]ethyl}-4-iodobenzamide (1).** Compound **1** was prepared from 4-iodobenzoyl chloride and 2,2′-(ethylenedioxy)bis(ethylamine). 4-Iodobenzoyl chloride (5.00 g, 18.8 mmol) in CH_2Cl_2 (125 mL) was added dropwise to 2,2′-(ethylenedioxy)bis(ethylamine) (22.2 g, 150 mmol) in CH_2Cl_2 (150 mL) and Et_3N (5 mL). The reaction mixture was stirred overnight and evaporated off. Water was added to the residue, and the resultant precipitate was filtered. The filtrate was extracted with EtOAc (400 mL). The organic layer was dried over $MgSO_4$ and evaporated off after filtration. The oily residue was solidified under vacuum. ^{1}H NMR (300 MHz, DMSO-d_6): δ 8.621 (t, 1H, J = 6.3 Hz), 7.82 (d, 2H, J = 8.4 Hz), 7.63 (d, 2H, J = 8.7 Hz), 4.25−3.45 (m, 6H), 3.59−3.33 (m, 4H), 2.64 (t, 2H, J = 5.7 Hz), 2.34 (bs, 2H). ^{13}C NMR (75 MHz, DMSO-d_6): 165.34, 136.94, 133.61, 129.01, 98.68, 72.90, 69.57, 69.47, 68.77, 41.31. HR-MS (ESI) calcd for $C_{13}H_{19}IN_2O_3$: 379.0513 (M^+ + H). Found: 379.0506 (M^+ + H), 401.0356 (M^+ + Na).

***N*-{2-[2-(2-Aminoethoxy)ethoxy]ethyl}-4-iodobenzamide (2).** 2-Chloropropinonyl chloride (0.71 g, 5.6 mmol) was added to compound **3** (2.0 g, 5.3 mmol) in a mixture of CH_2Cl_2 (20 mL) and Et_3N (0.74 mL, 5.3 mmol) in an ice bath. The reaction mixture was allowed to warm room temperature and stirred overnight. The solvent was evaporated off, and the crude product was purified by a silica gel chromatography (CH_2Cl_2 (95%)/MeOH (5%)) (2.3 g, 91%). ^{1}H NMR (300 MHz, $CDCl_3$): δ 7.88 (d, 2H, J = 6.6 Hz), 7.53 (d, 2H, J = 6.9 Hz), 6.98 (bs, 1H), 6.76 (bs, 1H), 4.44 (q, 1H, J = 7.2 Hz), 4.25−3.43 (m, 12H), 1.75 (d, 3H, J = 6.9 Hz). ^{13}C NMR (75 MHz, DMSO-d_6): 169.76, 166.88, 137.87, 133.99, 128.81, 98.71, 70.59, 70.54, 70.01, 69.71, 56.21, 40.18, 39.96, 23.07. HR-MS (ESI) calcd for $C_{16}H_{22}ClN_2O_4I$: 491.0205 (M^+ + H). Found: 469.0397 (M^+ + H), 491.0197 (M^+ + Na).

***N*-[2-(2-{2-[2-(*N*,*N*-Di-*tert*-butylaminooxy)propionylamino]ethoxy}ethoxy)ethyl]-4-iodobenzamide (3).** Compound **2** (300 mg, 0.640 mmol), Cu (61 mg, 0.96 mmmol), and CuCl (25 mg, 0.26 mmol) were placed in a 10 mL Schlenk flask and degassed by three quick cycles of vacuum and backfilling with Ar. Dioxane was Ar-purged for 10 min. Tris[2-(dimethylamino)ethyl]amine (Me_6TREN)[36] (59 mg, 0.26 mmol) in dioxane (3 mL) was poured into the Schenk flask, and di-*tert*-butylnitroxide (125 mg, 0.867 mmol) was added under Ar. The reaction mixture was stirred at 70 °C overnight. The reaction mixture was evaporated, and the residue was chromatographically separated by a gradient silica gel column (ethyl acetate (100%) to ethyl acetate (95%)/ethanol (5%)). The collected product was dissolved in CH_2Cl_2 and washed with saturated

NH_4Cl(aq) solution and saturated NaCl solution. The organic layer was dried over $MgSO_4$, and the solvent was evaporated off after a filtration of $MgSO_4$ to give an oily compound (190 mg, 61%). ^{1}H NMR (300 MHz, $CDCl_3$): δ 7.76 (d, 2H, J = 8.1 Hz), 7.53 (d, 2H, J = 8.7 Hz), 6.89 (bs, 2H), 4.31 (q, 1H, J = 6.9 Hz), 3.64−3.41 (m, 12H), 1.45 (d, 3H, J = 6.9 Hz), 1.21 (s, 18H). ^{13}C NMR (75 MHz, DMSO-d_6): 173.91, 166.77, 137.82, 134.03, 128.854, 98.65, 82.11, 70.55, 70.19, 70.05, 40.10, 38.90, 31.06, 30.61, 19.06. HR-MS (ESI) calcd for $C_{24}H_{40}IN_3O_5$: 600.1905 (M^+ + Na). Found: 578.2081 (M^+ + H), 600.1880 (M^+ + Na), 1177.3847 ($2M^+$ + Na).

Synthesis of PPE 6. Monomers **4** (87.3 mg, 0.0779 mmol), **5** (40.8 mg, 0.0909 mmol), and alkoxyamine **3** (10 mg, 0.0173 mmol) were placed in a 25 mL Schlenk flask. $Pd(PPh_3)_4$ (5%) and CuI (5%) were added to the flask in a glovebox. Morpholine was passed through an alumina column and degassed by three quick cycles of vacuum and backfilling with Ar before use. The solvent was cannulated into the flask containing the monomers (∼0.5 mL). The reaction mixture was degassed again and stirred at 60 °C overnight and poured into EtOAc. The precipitate was collected by centrifuge, washed with EtOAc and diethyl ether, and dried under vacuum. The compound was dissolved in water and dialyzed against water (Pierce, Snake skin, MWCO 3500) for 2 days (500 mL water × 4 times in a day). The polymer solution was then lyophilized (86 mg). ^{1}H NMR (300 MHz, DMSO-d_6): δ 7.75 (bs, 2H), 7.451 (bs, 2H), 7.074 (bs, 4H), 4.951 (bs, 16H), 4.596 (s, 8H), 4.098 (bs, 4H), 3.988 (bs, 4H), 3.560 (bs, 40H), 1.201 (s, 1.83H), 1.144 (s, 1.83H). DP = 11.5 by ^{1}H NMR. M_n = 23 556, M_w = 34 411, and PDI = 1.46 based on GPC analysis.

Synthesis of PPE−PolyNIPA Conjugate (P-I). PPE **6** (10 mg) and NIPA (500 mg) were placed in a 10 mL Schlenk flask and degassed by three cycles of vacuum and backfilling with Ar. Ar-purged DMF or DMSO (0.5 mL) was added to the flask by a syringe. The reaction mixture was stirred at 120 °C overnight. The polymer was precipitated in ethyl ether and collected by a centrifuge. The dried polymer was dissolved in water and purified by a dialysis against water. The polymer solution was then lyophilized after filtration to give a yellow powder (22 mg). M_n = 51 604, M_w = 233 100, and PDI = 4.52 based on GPC analysis.

Synthesis of RhB−PolyNIPA Conjugate (P-II). NIPA (0.50 g, 4.4 mmol), methacyloxyethyl thiocarbamoyl rhodamine B (7.4 mg, 0.011 mmol, Polysciences, Inc.), and AIBN (3.6 mg, 0.022 mmol) were placed in a 25 mL Schlenk tube and degassed by three vacuum−Ar filling cycles. Ar-purged DMF (1.5 mL) was added to the tube by a syringe. The reaction mixture was stirred at 60 °C overnight. The polymer was precipitated in ethyl ether and collected by a centrifuge and dried under vacuum. M_n = 86 909, M_w = 142 730, and PDI = 1.64 based on GPC analysis.

Synthesis of PPE−RhB−PolyNIPA Conjugate (P-III). PPE 6 (5 mg), NIPA (0.5 g), and methacyloxyethyl thiocarbamoyl rhodamine B (0.4 mg, 0.6 mmol, Polysciences, Inc.) were placed in a 25 mL Schlenk tube and degassed by three cycles of vacuum and backfilling with Ar. Ar-purged DMSO (0.5 mL) was added to the tube by a syringe. The reaction mixture was stirred at 120 °C overnight. The polymer was precipitated in ethyl ether and collected by centrifuge. The dried polymer was dissolved in water and purified by a dialysis against water (Pierce, Snake skin, MWCO 3500). The polymer solution was then lyophilized after filtration.

General Protocol for Thermally Induced Precipitation. Polymer stock solutions (20 mL) were prepared by stirring the polymers in deionized water and cooling in an ice bath. The polymer concentrations were 0.15 mg/mL for **P-I** and 0.25 mg/mL for **P-II** to give about 0.5 and 0.4 at the maximum in UV−vis absorbance, respectively. These polymer stock solutions were diluted to the desired concentration, and they were mixed to give polymer sample solutions. The sample solution (1 mL) was transferred to a 25 mL sample tube, and a saturated NaCl aqueous solution (0.1 mL) was added into the tube. The solution was heated at 50 °C in a water bath without stirring for 3 min. The resultant precipitate was vacuum-filtered with a filter paper (S&S filter paper, medium, pore size 8−12 μm, diameter 8 mm) on a Hirsch funnel and washed with a hot water (50 °C, 3 mL) without a salt. The filter paper was dried under vacuum overnight and placed between a coverslip and a glass microscope slide. Fluorescence from the collected precipitates on the filter paper was measured.

Acknowledgment. We thank the National Science Foundation through the Center for Materials Science and Engineering at MIT and NASA for financial support.

References and Notes

(1) McQuade, D. T.; Pullen, A. E.; Swager, T. M. *Chem. Rev.* **2000**, *100*, 2537−2574.
(2) (a) Yang, J. S.; Swager, T. M. *J. Am. Chem. Soc.* **1998**, *120*, 5321−5322. (b) Yang, J. S.; Swager, T. M. *J. Am. Chem. Soc.* **1998**, *120*, 11864−11873.
(3) Cumming, C. J.; Aker, C.; Fisher, M.; Fox, M.; la Grone, M. J.; Reust, D.; Rockley, M. G.; Swager, T. M.; Towers, E.; Williams, V. *IEEE Trans. Geosci. Remote Sensing* **2001**, *39*, 1119−1128.
(4) Liu, Y.; Mills, R. C.; Boncella, J. M.; Schanze, K. S. *Langmuir* **2001**, *17*, 7452−7455.
(5) Marsella, M. J.; Swager, T. M. *J. Am. Chem. Soc.* **1993**, *115*, 12214−12215.
(6) Wang, B.; Wasielewski, M. R. *J. Am. Chem. Soc.* **1997**, *119*, 12−21.
(7) Kim, J.; McQuade, D. T.; McHugh, S. K.; Swager, T. M. *Angew. Chem., Int. Ed.* **2000**, *39*, 3868−3872.
(8) Crawford, K. B.; Goldfinger, M. B.; Swager, T. M. *J. Am. Chem. Soc.* **1998**, *120*, 5187−5192.
(9) Gaylord, B. S.; Heeger, A. J.; Bazan, G. C. *Proc. Natl. Acad. Sci. U.S.A.* **2002**, *99*, 10954−10957.
(10) Gaylord, B. S.; Heeger, A. J.; Bazan, G. C. *J. Am. Chem. Soc.* **2003**, *125*, 896−900.
(11) Fan, C.; Plaxco, K. W.; Heeger, A. J. *J. Am. Chem. Soc.* **2002**, *124*, 5642−5643.
(12) Chen, L.; McBranch, D. W.; Wang, H.-L.; Helgeson, R.; Wudl, F.; Whitten, D. G. *Proc. Natl. Acad. Sci. U.S.A.* **1999**, *96*, 12287−12292.
(13) Ho, H. A.; Boissinot, M.; Bergeron, M. G.; Corbeil, G.; Doré, K.; Boudreau, D.; Leclerc, M. *Angew. Chem., Int. Ed.* **2002**, *41*, 1548−1551.
(14) Swager, T. M. *Acc. Chem. Res.* **1998**, *31*, 201−207.
(15) Wosnick, J. H.; Swager, T. M. *Curr. Opin. Chem. Biol.* **2000**, *4*, 715−720.
(16) Zhou, Q.; Swager, T. M. *J. Am. Chem. Soc.* **1995**, *117*, 7017−7018.
(17) McQuade, D. T.; Hegedus, A. H.; Swager, T. M. *J. Am. Chem. Soc.* **2000**, *122*, 12389−12390.
(18) Kimura, M.; Horai, T.; Hanabusa, K.; Shirai, H. *Adv. Mater.* **1998**, *10*, 459−462.
(19) Kuroda, K.; Swager, T. M. *Chem. Commun.* **2003**, 26.
(20) Schild, H. G. *Prog. Polym. Sci.* **1992**, *17*, 163−249.
(21) Matyjaszewski, K.; Woodworth, B. E.; Zhang, X.; Gaynor, S. G.; Matzner, Z. *Macromolecules* **1998**, *31*, 5955−5957.
(22) Hawker, C. J.; Bosman, A. W.; Harth, E. *Chem. Rev.* **2001**, *101*, 3661−3688.
(23) Stalmach, U.; de Boer, B.; Post, A. D.; van Hutten, P. F.; Hadziioannou, G. *Angew. Chem., Int. Ed.* **2001**, *40*, 428−430.
(24) Stalmach, U.; de Boer, B.; Videlot, C.; van Hutten, P. F.; Hadziioannou, G. *J. Am. Chem. Soc.* **2000**, *122*, 5464−5472.
(25) Benoit, D.; Chaplinski, V.; Braslau, R.; Hawker, C. J. *J. Am. Chem. Soc.* **1999**, *121*, 3904−3920.
(26) Ohno, K.; Tsujii, Y.; Miyamoto, T.; Fukuda, T.; Goto, M.; Kobayashi, K.; Akaike, T. *Macromolecules* **1998**, *31*, 1064−1069.
(27) Ohno, K.; Izu, Y.; Yamamoto, S.; Miyamoto, T.; Fukuda, T. *Macromol. Chem. Phys.* **1999**, *200*, 1619−1625.
(28) Jousset, S.; Hammouch, S. O.; Catala, J.-M. *Macromolecules* **1997**, *30*, 6685−6687.
(29) Harth, E.; Bosman, A. W.; Benoit, D.; Helms, B.; Fréchet, J. M. J.; Hawker, C. J. *Macromol. Symp.* **2001**, *174*, 85.

(30) Tsolakis, P. K.; Kallitsis, J. K.; Godt, A. *Macromolecules* **2002**, *35*, 5785.
(31) Freitag, R.; Garret-Flaudy, F. *Langmuir* **2002**, *18*, 3434−3400.
(32) Kim, J.; Swager, T. M. *Nature (London)* **2001**, *411*, 1030−1034.
(33) Monji, N.; Hoffman, A. S. *Appl. Biochem. Biotechnol.* **1987**, *14*, 107−120.
(34) Ding, Z.; Chen, G.; Hoffman, A. S. *Bioconjugate Chem.* **1996**, *7*, 121.
(35) Umeno, D.; Mori, T.; Maeda, M. *Chem. Commun.* **1998**, 1433−1434.
(36) Ciampolini, M.; Nardi, N. *Inorg. Chem.* **1966**, *5*, 41−44.

MA035373+